

Supersymmetric event generation

It is possible that the first indication of physics beyond the SM will come from indirect searches. These include direct or indirect detection of dark matter, $(g - 2)_\mu$, branching ratios (or event shapes) for various rare decays such as $B \rightarrow X_s \gamma$, $B \rightarrow X_s \ell^+ \ell^-$, $B_s \rightarrow \ell^+ \ell^-$ ($\ell = \mu, \tau$) or $\mu \rightarrow e \gamma$, or measurements of the electric dipole moment of the electron or the neutron. However, any such signal will likely be explainable by several new physics hypotheses, and not just supersymmetry. Thus, it is usually accepted that an unambiguous discovery of weak scale supersymmetry will have to occur at colliding beam experiments, where supersymmetric matter can be directly created, and the resultant scattering events can be scrutinized.

As we saw in Chapter 12 and Chapter 13, supersymmetric models can be used to predict various sparticle production rates and their subsequent decay patterns into final states containing quarks, leptons, photons, gluons (and LSPs in R -parity conserving models). However, quarks and gluons are never directly detected in any collider detector. Instead, detectors measure tracks of quasi-stable charged particles and their momenta as they bend in a magnetic field. They also measure energy deposited in calorimeter cells by hadrons, charged leptons, and photons. There is thus a gap between the predictions of supersymmetric models in terms of final states involving quarks, gluons, leptons and photons, and what is actually detected in the experimental apparatus. This gap is bridged by supersymmetric event generator computer programs. Once a collider type and supersymmetric model are specified, the event generator program can produce a complete simulation of the sorts of scattering events that are to be expected. The final state of any scattering event is composed entirely of electrons, muons, photons, and the long-lived hadrons (pions, kaons, nucleons, etc.) and their associated four-vectors that may be measured in a collider experiment.

The underlying idea of SUSY event generator programs is that for a specified collider type (e^+e^- , pp , $p\bar{p}$, ...) and center of mass energy, the event generator will, for any set of MSSM parameters, generate various sparticle pair production

events in the ratio of their production cross sections, and with distributions as given by their differential cross sections discussed in Chapter 12. Moreover, the produced sparticles will undergo a (possibly multi-step cascade) decay into a partonic final state, according to branching ratios as fixed by the model.¹ Finally, this partonic final state is converted to one that is comprised of particles that are detected in an experimental apparatus. By generating a large number of “SUSY events” using these computer codes, the user can statistically simulate the various final states that are expected to be produced within the framework of any particular model. Although we have been focussing upon supersymmetry, we should mention that these programs also allow the user to simulate SM processes. This is essential for assessing SM backgrounds to new physics.

Several event generator programs that incorporate SUSY are currently available, including ISAJET, PYTHIA, HERWIG, and SUSYGEN. These include the $2 \rightarrow 2$ leading order SUSY production processes discussed in Chapter 12. In addition, specific $2 \rightarrow n$ ($n \leq 6$) SUSY reactions may be generated by such programs as CompHEP, Madgraph-II, and GRACE. The output of these latter programs must then be interfaced with one of the event generator programs to yield complete scattering event simulations. Ideally, event generator programs should be flexible enough to enable simulation of SUSY events from a variety of models such as mSUGRA, GMSB, etc. In other words, the user should be able to use the input parameters of these specific models (instead of the MSSM parameters) and generate the corresponding scattering events at any collider. In this way, different hypotheses about how MSSM superpartners obtain their masses may be directly tested by experiments at colliding beam facilities. In this connection, we also note that publicly available programs such as ISAJET, SPheno, SuSpect, and SOFTSUSY can be used to evaluate weak scale MSSM parameters and sparticle masses for several of the models that we have discussed in Chapter 11. Other than ISAJET, these programs do not generate sparticle production events, although the program SPheno will generate a table of sparticle decay branching fractions.

The simulation of hadron collider scattering events may be broken up into several steps, as illustrated in Fig. 14.1. The steps include:

- the perturbative calculation of the hard scattering subprocess in the parton model, and convolution with parton distribution functions (PDFs), as encapsulated by (12.1);
- inclusion of sparticle cascade decays;

¹ The user usually has the option to generate only a subset of SUSY production reactions or decays. This is useful if one wants to focus on a signal in a particular channel.

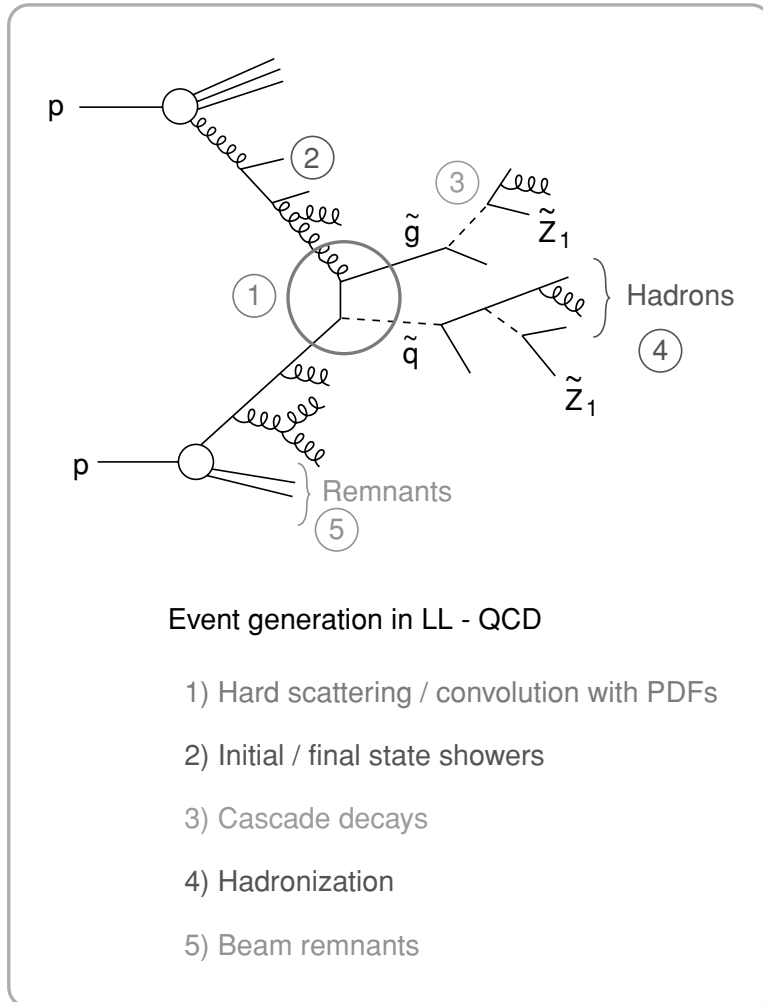


Figure 14.1 Steps in any event generation procedure.

- implementation of perturbative parton showers for initial and final state colored particles, and for other colored particles which may be produced as decay products of heavier objects;
- implementation of a hadronization model which describes the formation of mesons and baryons from quarks and gluons. Also, unstable particles must be decayed to the (quasi-)stable daughters that are ultimately detected in the apparatus, with rates and distributions in accord with their measured or predicted values.
- Finally, the debris from the colored remnants of the initial beams must be modeled to obtain a valid description of physics in the forward regions of the collider detector.

Some of these steps are absent for simulations of electron–positron collisions which, as we saw in Chapter 12, are intrinsically simpler. However, for e^+e^- collider simulations, we have to allow for polarized initial beams.

In this chapter, we first briefly describe the physics involved in each of these steps. We then outline how this has been incorporated into some of the available event generator programs. Special attention is paid to the program ISAJET, since we have been involved with its development for describing supersymmetric processes.

14.1 Event generation

14.1.1 Hard scattering

The hard scattering and convolution with parton distributions forms the central calculation of event generator programs. The calculations are usually performed at lowest order in perturbation theory, so that the hard scattering is either a $2 \rightarrow 2$ or $2 \rightarrow 1$ scattering process.

For supersymmetric particle production at a high energy hadron collider such as the LHC, a large number of hard scattering subprocesses are likely to be kinematically accessible. Each subprocess reaction must be convoluted with parton distribution functions so that a total cross section for each reaction may be determined. The Q^2 -dependent PDFs commonly used are constructed to be solutions of the Dokshitzer, Gribov, Lipatov, Altarelli, Parisi (DGLAP) QCD evolution equations, which account for multiple *collinear* emissions of quarks and gluons from the initial state in the leading log approximation. As Q^2 increases, more gluons are radiated, so that the distributions soften for large values of x , and correspondingly increase at small x values. Use of a running QCD coupling constant makes the entire calculation valid at leading log level.

Once the total cross sections are evaluated for all the allowed subprocesses, then reactions may be selected probabilistically (with an assigned weight) using a random number generator. This will yield sparticle events in the ratio predicted by the particular model being simulated.

For sparticle production at e^+e^- colliders, it may also be necessary to convolute with PDFs to incorporate bremsstrahlung and beamstrahlung effects as described in Chapter 12. In addition, if beam polarization is used, then each subprocess cross section will depend on beam polarization parameters as well.

14.1.2 Parton showers

For reactions occurring at both hadron and lepton colliders, to obtain a realistic portrait of supersymmetric (or Standard Model) events, it is necessary to account for multiple *non-collinear* QCD radiation effects. The evaluation of the cross section

using matrix elements for multi-parton final states is prohibitively difficult. Instead, these multiple emissions are approximately included in an event simulation via a parton shower (PS) algorithm.² They give rise to effects such as jet broadening, radiation in the forward regions and energy flow into detector regions that are not described by calculations with only a limited number of final state partons.

In leading log approximation (LLA), the cross section for *single* gluon emission from a quark line is given by

$$d\sigma = \sigma_0 \frac{\alpha_s}{2\pi} \frac{dt}{t} P_{qq}(z) dz, \quad (14.1)$$

where σ_0 is the overall hard scattering cross section, t is the intermediate state virtual quark mass, and $P_{qq}(z) = \frac{4}{3} \left(\frac{1+z^2}{1-z} \right)$ coincides with the Altarelli–Parisi splitting function for $q' \rightarrow qg$ for the fractional momentum of the final quark $z \equiv |\vec{p}_q|/|\vec{p}_{q'}| < 1$. Interference between various *multiple* gluon emission Feynman graphs, where the gluons are ordered differently, is a subleading effect which can be ignored. Thus, Eq. (14.1) can be applied successively, and gives a factorized probability for each gluon emission. The idea behind the PS algorithm is then to use these approximate emission probabilities (which are exact in the collinear limit), along with exact (non-collinear) kinematics to construct a program which describes multiple non-collinear parton emissions. Notice, however, that the cross section (14.1) is singular as $t \rightarrow 0$ and as $z \rightarrow 1$, i.e. in the regime of collinear and also soft gluon emission. These singularities can be regulated by introducing physically appropriate cut-offs. A cut-off on the value of $|t|$ of order $|t_c| \sim 1$ GeV corresponds to the scale below which QCD perturbation theory is no longer valid. A cut-off on z is also necessary, and physically corresponds to the limit beyond which the gluon is too soft to be resolved.

The PS algorithms available vary in their degree of sophistication. The simplest algorithm was created by Fox and Wolfram in 1979. Their method was improved to account for interference effects in the angle-ordered algorithm of Marchesini and Webber. In addition, parton emission from heavy particles results in a dead-cone effect, where emissions in the direction of the heavy particle are suppressed. Furthermore, it is possible to include spin correlations in the PS algorithm.

PS algorithms are also applied to the initial state partons. In this case, a backwards shower algorithm is most efficient, which develops the emissions from the hard scattering backwards in time towards the initial state. The backward shower algorithm developed by Sjöstrand makes use of the PDFs evaluated at different energy scales to calculate the initial state parton emission probabilities.

² For more detailed discussions beyond the scope of this text, see e.g. *Collider Physics*, V. Barger and R. J. N. Phillips, Addison-Wesley (1987), Chapter 9.

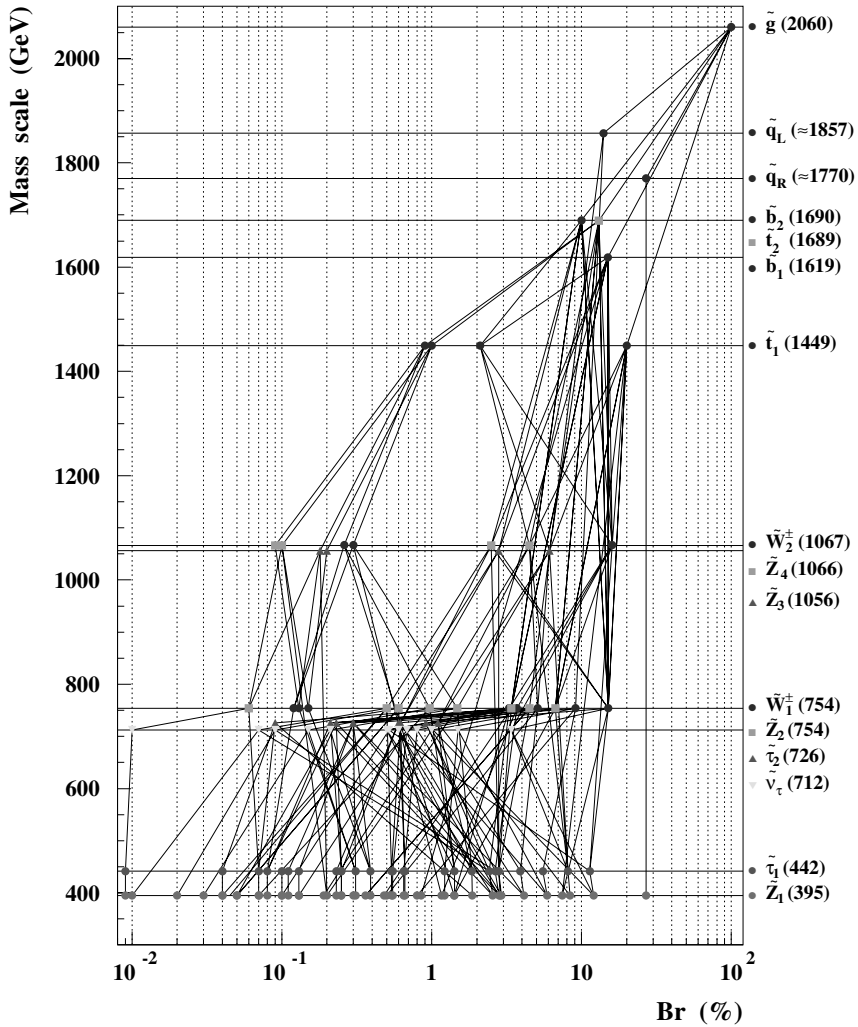
14.1.3 Cascade decays

We have already seen that not only are there many reactions available via which SUSY particles may be produced at colliders but, once produced, there exist many ways in which superparticles may decay. For the next-to-lightest SUSY particle (NLSP), there may be only one or at most a few ways to decay to the LSP. Thus, for a collider such as LEP or even the Fermilab Tevatron, where only the lightest sparticles will have significant production rates, we might expect that their associated decay patterns will be relatively simple. However, the number of possible final states increases rapidly if squarks and gluinos that can decay into the heavier charginos and neutralinos are accessible, and the book-keeping becomes correspondingly more complicated. Indeed, at the CERN LHC, where the massive strongly interacting sparticles such as gluinos and squarks are expected to be produced at large rates, sparticle cascade decay patterns can be very complex.³ As an example, the many possible decay paths of a gluino in the mSUGRA model are shown in Fig. 14.2. Branching fractions to a variety of final states resulting from the cascade decay are also listed in the figure.

Monte Carlo event generators immensely facilitate the analysis of signals from such complex cascade decays, especially in the case where no single decay chain dominates. An event generator can select different cascade decay branches by generating a random number which picks out a particular decay choice, with a weight proportional to the corresponding branching fraction, at each step of the cascade decay. Quarks and gluons produced as the end products of cascade decays will shower off still more quarks and gluons, with probabilities determined by the PS algorithm.

The procedure that we have just described is exact for cascade decays of spinless particles into two other spinless particles at each step in the cascade. This is because the squared matrix element is just a constant, and there are no spin correlations possible. This is not true in general and in some cases it can be very important to include the decay matrix element and/or spin correlations in the calculation of cascade decays of sparticles. For instance, it has been suggested that the end point of the dilepton mass distribution from $\tilde{W}_1 \tilde{Z}_2 \rightarrow q\bar{q}'\tilde{Z}_1 + \ell\bar{\ell}\tilde{Z}_1$ production at hadron colliders yields a good measure of $m_{\tilde{Z}_2} - m_{\tilde{Z}_1}$. Frequently, interference between Z and slepton mediated amplitudes for \tilde{Z}_2 decays suppresses this mass distribution near the kinematic end point, leading to greater uncertainties in its determination relative to the expectation with a constant matrix element. As an extreme example of the distortion due to effects from the decay matrix element, in Fig. 14.3 we show this distribution for $\tilde{W}_1 \tilde{Z}_2$ events at the Fermilab Tevatron collider for the choice of mSUGRA parameters ($m_0, m_{1/2}, A_0, \tan\beta, \text{sign}(\mu)$) shown on the figure. For this

³ H. Baer, V. Barger, D. Karatas and X. Tata, *Phys. Rev.* **D36**, 96 (1987).



\tilde{Z}_1 qq	(27.0 %)	\tilde{Z}_1 $\tau\nu$ WWbb	(4.1 %)
\tilde{Z}_1 $\tau\nu$ Wbb	(12.1 %)	\tilde{Z}_1 $\tau\tau$ bb	(2.9 %)
\tilde{Z}_1 $\tau\tau$ WWbb	(8.4 %)	\tilde{Z}_1 $\tau\tau$ qq	(2.9 %)
\tilde{Z}_1 WWbb	(7.4 %)	\tilde{Z}_1 $\tau\nu$ ZWbb	(2.8 %)
\tilde{Z}_1 $\tau\nu$ qq	(5.9 %)	\tilde{Z}_1 $\tau\nu$ hWbb	(2.6 %)

Figure 14.2 An illustration of the branching fraction for various cascade decays of the gluino within the mSUGRA model with parameters $m_0 = 400$ GeV, $m_{1/2} = 900$ GeV, $\tan \beta = 35$, $A_0 = 0$, and $\mu > 0$. The masses of various sparticles are also shown. This figure is adapted from S. Abdullin and D. Denegri, hep-ph/9905510.

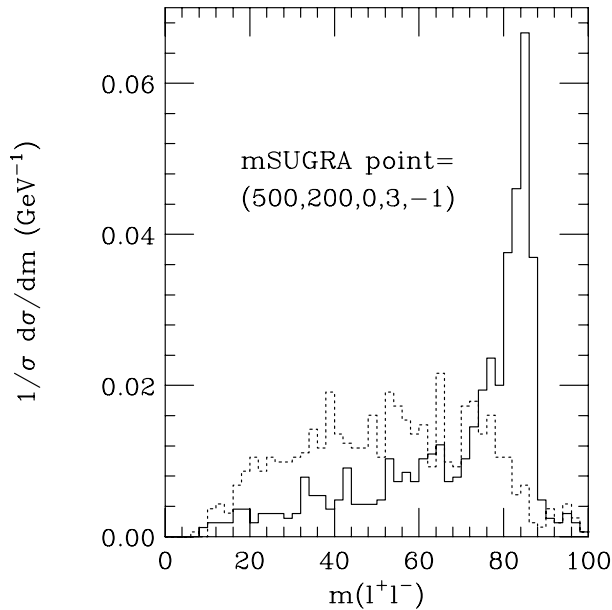


Figure 14.3 Distribution of opposite sign, same flavor dileptons from $\tilde{W}_1 \tilde{Z}_2$ production at the Fermilab Tevatron. The solid histogram shows the distribution including the exact matrix element, while the dashed histogram is the same distribution assuming that the decay matrix element is constant. Reprinted with permission from H. Baer, M. Drees, F. Paige, P. Quintana and X. Tata, *Phys. Rev.* **D61**, 095007 (2000), copyright (2000) by the American Physical Society.

parameter space point, $m_{\tilde{Z}_2} = 173$ GeV and $m_{\tilde{Z}_1} = 86$ GeV so one expects a dilepton mass distribution cut-off at $m_{\tilde{W}_1} - m_{\tilde{Z}_1} = 87$ GeV. The dilepton mass distribution including decay matrix element energy effects is denoted by the solid histogram, and is highly distorted by the pole of the virtual Z boson in the decay diagrams relative to the distribution using just phase space for the \tilde{Z}_2 decay (dashed histogram).

Spin correlation effects are especially important for precision measurements at e^+e^- linear colliders. While retaining spin correlations may be less crucial in many situations at a hadron collider, this is not always the case. For instance, relativistic τ^- leptons produced from W decay are always left-handed, while those produced from a charged Higgs decay are always right-handed. Likewise, the polarization of the taus from $\tilde{\tau}_1$ decays depends on the stau mixing angle. Since the undetectable energy carried off by ν_τ from tau decay depends sensitively on the parent tau helicity, it is necessary to include effects of tau polarization in any consideration involving the energy of “tau jets”.⁴ By evaluating the mean polarization of taus in any particular

⁴ These effects are crucial for assessing the efficiency for identifying hadronically decaying taus at a hadron collider.

process, these effects can be incorporated, at least on average, into event generator programs. Of course, such a procedure would not include correlations between decay products of two taus produced in the same reaction.

14.1.4 Models of hadronization

Once sparticles have been produced and have decayed through their cascades, and parton showers have been evolved up to the point where the partons have virtuality smaller than $\sim 1 \text{ GeV}^2$, we have to convert these to hadrons. This is a non-perturbative process, and we have to appeal to phenomenological models for its description. The independent hadronization (IH) model of Field and Feynman is the simplest such model to implement. In this picture, a new quark–antiquark pair $q_1\bar{q}_1$ can be created in the color field of the parent quark q_0 . Then the $q_0\bar{q}_1$ pair can turn into a meson with a longitudinal momentum fraction described by a phenomenological function, with the remainder of the longitudinal momentum carried by the quark q_1 . This process is repeated by the creation of a $q_2\bar{q}_2$ pair in the color field of q_1 , and so on down the line to $q_n\bar{q}_n$. A host of mesons are thus produced, and decayed to the quasi-stable π , K , . . . mesons according to their experimental properties. The final residual quark q_n will have very little energy, and can be discarded without significantly affecting jet physics. Finally, a small transverse momentum can be added according to a pre-assigned Gaussian probability distribution to obtain a better description of the data. Quark fragmentation into baryons is also possible by creation of diquark pairs in its color field, and can be incorporated. The IH scheme will thus describe the bulk features of hadronization needed for event simulation programs.

The string model of hadronization developed at Lund is a more sophisticated model than IH, which treats hadron production as a universal process independent of the environment of the fragmenting quark. In the string model, a produced quark–antiquark pair is assumed to be connected by a color flux tube or string. As the quark–antiquark pair moves apart, more and more energy is stored in the string until it is energetically favorable for the string to break, creating a new quark–antiquark pair. Gluons are regarded as kinks in the string. The string model correctly accounts for color flow in the hadronization process, as opposed to the IH model. In $e^+e^- \rightarrow q\bar{q}g$ (3-jet) events, the string model predicts fewer produced hadrons in the regions between jets than the IH model, in accord with observation.

A third scheme for hadronization is known as the cluster hadronization model. In this case, color flow is still accounted for, but quarks and antiquarks that are nearby in phase space will form a cluster, and will hadronize according to preassigned probabilities. This model avoids non-locality problems associated with the string hadronization model, where quarks and antiquarks separated by spacelike distances can affect the hadronization process.

14.1.5 Beam remnants

Finally, at a hadron collider the colored remnants of the nucleon that did not participate in the hard scattering must be accounted for. These beam remnant effects produce additional energy flow, especially in the far forward regions of the detector. A variety of approaches are available to describe these non-perturbative processes, including models involving Pomeron exchange and multiple scatterings. In addition, the beam remnants must be hadronized as well, and appear to require a different parametrization from “minimum bias” events where there are only beam jets but no hard scattering.

14.2 Event generator programs

Publicly available event generators for SUSY processes include

- **ISAJET:** (H. Baer, F. Paige, S. Protopopescu and X. Tata),
<http://www.phy.bnl.gov/~isajet/>
- **PYTHIA:** (T. Sjöstrand, L. Lönnblad and S. Mrenna),
<http://www.thep.lu.se/~torbjorn/Pythia.html>
- **HERWIG:** (G. Corcella, I. G. Knowles, G. Marchesini, S. Moretti, K. Odagiri, P. Richardson, M. Seymour and B. R. Webber),
<http://hepwww.rl.ac.uk/theory/seymour/herwig/>
- **SUSYGEN:** (N. Ghodbane, S. Katsanevas, P. Morawitz and E. Perez),
<http://lyoinfo.in2p3.fr/susygen/susygen3.html>

The event generator program ISAJET was originally developed in the late 1970s to describe scattering events at the ill-fated ISABELLE pp collider at Brookhaven National Laboratory. It was developed by F. Paige and S. Protopopescu to generate SM and beyond scattering events at hadron colliders and, to a lesser extent, e^+e^- colliders. ISAJET was the first event generator program developed to give a realistic portrayal of SUSY scattering events. ISAJET uses the IH model for hadronization, and the original Fox–Wolfram (Sjöstrand) PS shower algorithm for final state (initial state) parton showers. It includes an n -cut Pomeron model to describe beam-jet evolution.

The event generator PYTHIA was developed mainly by T. Sjöstrand in the early 1980s to implement the Lund string model for event generation. S. Mrenna contributed the inclusion of SUSY processes in PYTHIA.

The event generator HERWIG was developed in the mid-1980s to describe scattering events with angle-ordered parton showers, which accounted for interference effects neglected in the Fox–Wolfram shower approach. HERWIG implements

a cluster hadronization model. Supersymmetric processes are now available in HERWIG.

The program SUSYGEN was developed by S. Katsanevas and others to generate $e^+e^- \rightarrow$ SUSY events for the LEP experiments. SUSYGEN interfaces with PYTHIA for hadronization and showering. SUSYGEN has since been upgraded to also generate events for hadron colliders.

A description of these codes, or a comparison of their relative virtues and shortcomings, is beyond the scope of this text. Moreover, any such discussion would rapidly become out of date as these programs are continually being upgraded. We refer the interested reader to the webpages cited above, both for how to use these codes, and also for a description of the physics underlying these event generators.

We have already noted that in addition to these event generator codes, there are several specialized codes (SPHeno, SuSpect, SOFTSUSY) for the evaluation of sparticle spectra. In addition, there are publicly available codes for a careful evaluation (including loop effects) of the mass spectrum (FeynHiggs, FeynHiggsFast) and decay rates (HDECAY) of MSSM Higgs bosons. A careful evaluation of these is especially useful because, as we saw in Chapter 8, m_h is bounded above in a wide class of models, and experiments searching for a signal for h have already excluded significant portions of its allowed range.⁵ Finally, we note that $2 \rightarrow n$ (with $n \leq 6$) hard scattering processes including SUSY particles may be generated by programs such as CompHEP (E. Boos *et al.*), Madgraph-II (T. Stelzer and W. F. Long), and GRACE (Minami–Tateya Collaboration, M. Jimbo *et al.*). These codes need to be interfaced with one of the event generators, and are especially useful if specific reactions need to be generated including, for instance, effects of spin correlations.

14.3 Simulating SUSY with ISAJET

In this section, we illustrate the use of SUSY event generators using ISAJET (with which we are most familiar) as an example. The interested reader can follow similar procedures for any of the other event generator codes.

14.3.1 Program set-up

ISAJET is a publicly available code, and can be obtained from the website <http://www.phy.bnl.gov/~isajet/>. ISAJET is written in Fortran 77, and the code is maintained by the Patchy code management system, which is included in the CERLIB library of subroutines. The files available are

⁵ We stress that one should interpret the excluded region with care, since it is sensitive to underlying assumptions. For instance, if MSSM parameters are complex, the excluded mass range may be significantly smaller.

`isajet.car` and a Unix `Makefile`. The `Makefile` program must be edited to suit the user's particular machine. Running the `Makefile` on `isajet.car` creates a number of programs, including `isasugra.x`, `isasusy.x`, `isajet.x`, and `isajet.tex`. The last is a LaTeX file of the ISAJET manual.⁶

The program `isasusy.x` requires a weak scale MSSM parameter set as its input, and produces an output file with the corresponding physical sparticle masses along with (s)particle decay rates and branching fractions. The program `isasugra.x` accepts as an input parameters from the various SUSY breaking models described in Chapter 11, including SUGRA models with universal or non-universal SSB terms, GMSB models and AMSB models, and models including right-handed neutrinos ν_R . The program then uses the RGEs discussed in Chapter 9 to evolve these parameters, which are typically specified at some high scale, down to the weak scale relevant for phenomenology. These weak scale parameters are then used to evaluate the sparticle masses, decay rates and decay branching fractions which are written to a user-readable output file. The outputs of either `isasusy.x` or `isasugra.x` serve as input parameters for the program `isajet.x` which actually generates SUSY events corresponding to the particular model under study.

14.3.2 Models for SUSY in ISAJET

MSSM

The program `isasusy.x` calculates weak scale sparticle masses and their associated branching fractions in terms of a subset of weak scale MSSM input parameters. The relevant input parameters include:

$$m_t \quad (14.2a)$$

$$m_{\tilde{g}}, \mu, m_A, \tan \beta \quad (14.2b)$$

$$m_{Q_{11}}, m_{D_{11}}, m_{U_{11}}, m_{L_{11}}, m_{E_{11}} \quad (14.2c)$$

$$m_{Q_{33}}, m_{D_{33}}, m_{U_{33}}, m_{L_{33}}, m_{E_{33}}, (A_u)_{33}, (A_d)_{33}, (A_\tau)_{33} \quad (14.2d)$$

plus optional inputs of

$$m_{Q_{22}}, m_{D_{22}}, m_{U_{22}}, m_{L_{22}}, m_{E_{22}} \quad (14.2e)$$

$$M_1, M_2 \quad (14.2f)$$

$$m_{3/2} \quad (14.2g)$$

ISAJET currently takes the soft-SUSY breaking sfermion mass squared matrices to be real and diagonal; also, only third generation diagonal trilinear A terms

⁶ The ISAJET manual is also available on the hep-ph archive as H. Baer, F. Paige, S. Protopopescu and X. Tata, hep-ph/0001086.

are allowed. This corresponds to the simplified parameter space discussed in Section 8.1.2. If the optional second generation masses are not specified, then their values are set equal to the corresponding first generation masses. Also, the $U(1)_Y$ and $SU(2)_L$ gaugino masses are fixed by the gaugino mass unification relation

$$\frac{M_1}{\alpha_1} = \frac{M_2}{\alpha_2} = \frac{M_3}{\alpha_3} \quad (14.3)$$

unless the optional independent gaugino masses are specified. Finally, if the value of $m_{3/2}$ is not specified, it is assumed that the gravitino is heavy enough so that it effectively decouples from particle phenomenology.

The Higgs boson masses are computed using the RG improved one-loop effective potential evaluated at an optimized scale choice $Q = \sqrt{m_{\tilde{t}_L} m_{\tilde{t}_R}}$: using this high scale effectively accounts for some of the larger two-loop effects.

mSUGRA

For the mSUGRA model included in `isasugra.x`, the model inputs are

$$m_0, m_{1/2}, A_0, \tan \beta, \text{sign}(\mu), \text{ and } m_t. \quad (14.4)$$

Then ISAJET calculates the gauge and third generation Yukawa couplings at the weak scale in the \overline{DR} scheme, and evolves the set of six gauge and Yukawa couplings via two-loop RGEs up to the GUT scale, which is defined as the Q value at which $g_1 = g_2$. At the scale M_{GUT} , all SSB scalar masses are set to m_0 , all gaugino masses are set to $m_{1/2}$ and all third generation diagonal trilinear A terms are set to A_0 . Then the set of 26 MSSM couplings and parameters are evolved via two-loop RGEs to the weak scale. More precisely, each SSB term is frozen out at the scale equal to its absolute value, except for Higgs sector parameters, which are frozen at $Q = \sqrt{m_{\tilde{t}_L} m_{\tilde{t}_R}}$. One-loop corrections are added to the scalar potential, which is then minimized to obtain the value of μ^2 and $B(Q)$, consistent with radiative breaking of electroweak symmetry with the correct value of M_Z . SUSY threshold corrections to m_t , m_b , and m_τ , which considerably modify the relation between SM fermion masses and the corresponding Yukawa couplings if $\tan \beta$ is large, are computed at this stage. The set of couplings and mass parameters are then evolved iteratively between M_{GUT} and M_{weak} until the solution to the RGEs converges to within a specified tolerance.

Non-universal SUGRA

To facilitate simulation of models with non-universal gaugino masses, or models with non-universal scalar masses (e.g. models with additional D -term contributions, or gaugino-mediated SUSY breaking models), ISAJET includes the “Non-universal

SUGRA” option which allows the user to set arbitrary values of the SSB parameters

$$M_1, M_2, M_3 \quad (14.5a)$$

$$A_t, A_b, A_\tau \quad (14.5b)$$

$$m_{H_d}, m_{H_u} \quad (14.5c)$$

$$m_{Q_{11}}, m_{D_{11}}, m_{U_{11}}, m_{L_{11}}, m_{E_{11}} \quad (14.5d)$$

$$m_{Q_{33}}, m_{D_{33}}, m_{U_{33}}, m_{L_{33}}, m_{E_{33}} \quad (14.5e)$$

at $Q = M_{\text{GUT}}$, in place of the universal scalar mass and the universal A -parameter of the mSUGRA model. First and second generation SSB scalar masses are assumed equal. As in mSUGRA, these serve as boundary conditions for the RGEs which are again used to evaluate the weak scale values of MSSM SSB parameters from which sparticle masses, couplings, and decay branching fractions are obtained. The user also has the option to specify the scale Q at which the boundary conditions are to be implemented, allowing more accurate simulation of string-based scenarios.

GMSB models

ISAJET also allows for event generation in a variety of GMSB models. The set (11.39) of parameters of the mGMSB model

$$\Lambda, M, n_5, \tan \beta, \text{sign}(\mu), C_{\text{grav}} \quad (14.6a)$$

can directly be used as an input to ISAJET. As in mSUGRA, the gauge and Yukawa couplings at the weak scale are first evolved up in energy to $Q = M$, the messenger scale, where the calculated GMSB SSB mass parameters are used as boundary conditions for the RGEs. All parameters are then evolved back down to the weak scale, where the scalar potential is minimized and REWSB is imposed as usual.

ISAJET also allows event generation of many non-minimal GMSB models, by allowing several additional input parameters:

$$\mathcal{R}, \delta m_{H_d}^2, \delta m_{H_u}^2, D_Y(M), n_5(1), n_5(2), n_5(3). \quad (14.6b)$$

In this set, \mathcal{R} is a gaugino mass multiplier that decouples gaugino and scalar mass parameters at the messenger scale. This can occur if the scale for a $U(1)_R$ symmetry breaking differs from the SUSY breaking scale. For the minimal model, $\mathcal{R} = 1$. The parameters $\delta m_{H_d}^2$ and $\delta m_{H_u}^2$ are additional contributions to the Higgs SSB masses at the messenger scale which may arise from additional interactions that generate the dimensional B and μ parameters. These additional contributions are zero in the mGMSB model. In (14.6b), $D_Y(M)$ is the VEV of the hypercharge D -term in the messenger sector, and can lead to additional contributions $\delta m^2(M) = g' Y D_Y(M)$ to scalar mass parameters at $Q = M$. Finally, allowing incomplete

messenger representations can effectively yield differing numbers of messengers ($n_{5_1}, n_{5_2}, n_{5_3}$) for each factor of the gauge group.

AMSB models

ISAJET also has the minimal anomaly-mediated SUSY breaking model hardwired. It accepts the mAMSB parameter set

$$m_0, m_{3/2}, \tan \beta, \text{sign}(\mu), \quad (14.7)$$

as an input, and then evolves gauge and Yukawa couplings to M_{GUT} , where the mAMSB SSB masses are imposed as boundary conditions for the RGEs. The complete set of SSB masses and couplings are evolved to the weak scale where REWSB is imposed as usual.

Models with right-handed neutrinos

ISAJET allows the simulation of models with right-handed neutrino (RHN) superfields that are so topical today. In addition to other parameters, the user has to specify (see (9.37)),

$$M(\nu_3), M_N, A_\nu, m_{\tilde{\nu}_R}, \quad (14.8)$$

where $M(\nu_3)$ is the third generation neutrino mass, M_N is the heavy mass in the neutrino see-saw, A_ν is the new third generation neutrino trilinear A -parameter and $m_{\tilde{\nu}_R}$ the SSB mass of the RHNs. The parameter B_ν in (9.37) only affects the mass of the very heavy right-handed sneutrinos, and so is irrelevant for our purposes. As for other fermions, the masses and Yukawa couplings of the first two generations of neutrinos are neglected. Typically, we expect that $M_N \sim M_{\text{GUT}}$, while A_ν and $m_{\tilde{\nu}_R}$ are comparable to the weak scale. If one inputs a value of $M(\nu_3) = 0$, then ISAJET computes the third generation neutrino Yukawa coupling f_ν by imposing $f_\nu = f_t$ at M_{GUT} , as expected in $SO(10)$ SUSYGUT models.

14.3.3 Generating events with ISAJET

The programs `isasusy` and `isasugra` are useful for examining sparticle masses and branching fractions expected in different models. For generating collider events, `isajet` must be used. `isajet` takes its input from an input parameter file such as the file `sugra.par` as shown below. This file implements sparticle production events for the Fermilab Tevatron $p\bar{p}$ collider at $\sqrt{s} = 2$ TeV.

```
TEST SUGRA JOB
2000,5000,0,0/
SUPERSYM
```

```

BEAMS
'P', 'AP' /
SEED
9998871/
NTRIES
5000/
SUGRA
100,200,0,3,1/
TMASS
175,-1,-1/
JETTYPE1
'ALL' /
JETTYPE2
'ALL' /
PT
10,250,10,250/
END
STOP

```

The first line is a comment line, containing the job title. The second line is the collider CM energy, the number of events to be generated, the number of events to print out, and the number of events to skip between printing. The third line gives the class of reactions: in this case, supersymmetric ones. The fourth and fifth lines denote the beam types: here proton and antiproton. The fifth and sixth lines specify a random seed for event generation; by altering the seed, an independent set of events can be generated. NTRIES on the next two lines limits the number of tries (in this case, 5000) that the program makes to find a good event. The tenth line denotes the SUGRA model inputs (m_0 , $m_{1/2}$, A_0 , $\tan \beta$, sign (μ)) specified on the next line. Lines 12–13 show the top quark mass input, while lines 14–15 specify the types of sparticles to be produced in the $2 \rightarrow 2$ subprocess: in this case, all allowed reactions will occur. By limiting JETTYPE1 and JETTYPE2 to be specific sparticle(s), particular (sets of) SUSY reactions can be studied. Lines 18–19 show the p_T range of the final state particles in the $2 \rightarrow 2$ hard scattering process. Finally, the last two lines indicate the end of the file.

For generating scattering events at an e^+e^- linear collider, the input might look like this:

```

TEST SUGRA JOB FOR A LC WITH BEAM POLARIZATION
      AND BEAMSTRAHLUNG
500,5000,0,0/

```



```

E+E-
SEED
9998871/
NTRIES
5000/
SUGRA
2375,300,0,30,1/
EPOL
0.9,0/
EBEAM
400,500,.1072,.12/
TMASS
175,-1,-1/
JETTYPE1
'ALL'/
JETTYPE2
'ALL'/
END
STOP

```

In the above file, e^+e^- events are stipulated by the E+E- reaction card on line 3. Since the SUGRA model is stipulated, `isajet` will generate SUSY events. On lines 10–11, a left-polarized electron beam with $P_L(e^-) = 0.9$ is stipulated to scatter from an unpolarized positron beam. In lines 12–13, beamstrahlung is enabled, and the reaction subprocess energy is restricted to lie between 400–500 GeV. The beamstrahlung parameters $\Upsilon = 0.1072$ and $\sigma_z = 0.12$ mm (as defined in Section 12.2.4) must also be given.

There are several ISAJET output files. One will include various masses, and the sum total of all cross sections generated. Another will include the actual scattering events, which consists of dumping out various ISAJET common blocks, including PARTCL, which contains all final state particles, their identities, sources, and four-vectors. This output is in a form suitable for analysis, or for interface with detector simulation programs. Further details along with program updates can be found in the ISAJET manual, `isajet.tex`.

As an example of a supersymmetric scattering event, we show in Fig. 14.4 a $pp \rightarrow \tilde{g}\tilde{u}_L X$ event generated within the mSUGRA framework for the CMS detector at the CERN LHC collider with $\sqrt{s} = 14$ TeV. The response of various detector elements to the passage of particles through them was simulated by the program GEANT. The mSUGRA model parameters are also shown in the figure, along with several sparticle masses and the sparticle cascade decay chains. Six high E_T jets,

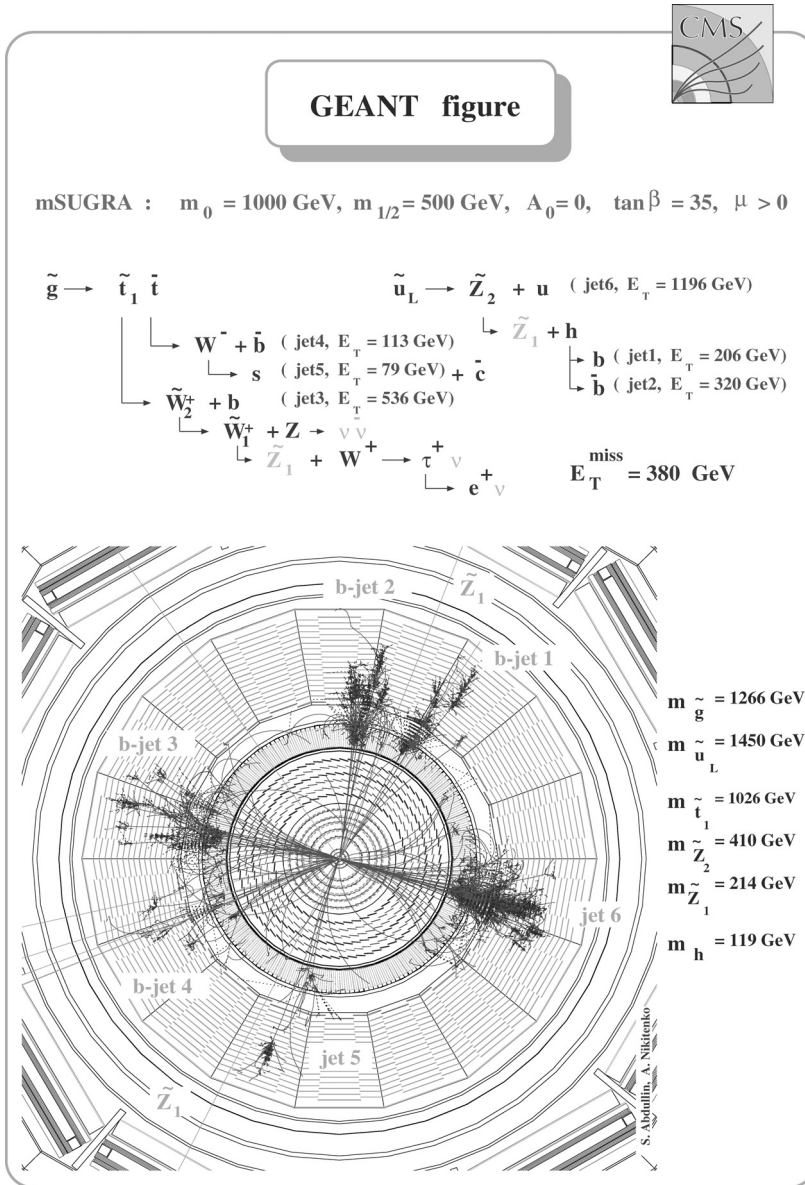


Figure 14.4 GEANT simulation of an ISAJET mSUGRA event for the CMS detector at the CERN LHC. Notice the large multiplicity of *b*-jets. Adapted from a figure, courtesy of Salavat Abdullin.

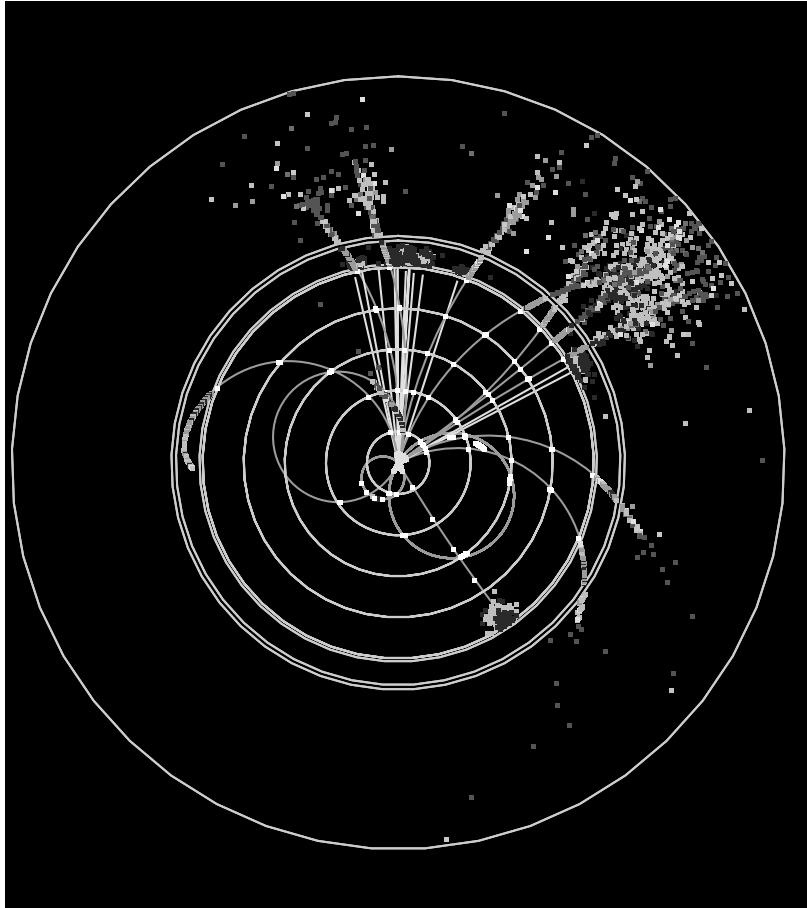


Figure 14.5 Simulated chargino pair production event using ISAJET, within the framework of the mSUGRA model with parameters $m_0 = 2375$ GeV, $m_{1/2} = 300$ GeV, $A_0 = 0$, $\tan \beta = 30$, and $\mu > 0$. The parameter space point is in the focus point region, and gives $\Omega_{\tilde{Z}_1} h^2 = 0.11$, consistent with WMAP measurements. The simulated reaction is $e^+e^- \rightarrow \tilde{W}_1^+ \tilde{W}_1^- \rightarrow u\tilde{d}\tilde{Z}_1 + e\tilde{\nu}_e\tilde{Z}_1$ at a $\sqrt{s} = 500$ GeV linear collider. Figure courtesy of Norman Graf.

the hardest with $E_T = 1196$ GeV and the softest with $E_T = 79$ GeV, result from these cascade decays. Moreover, four of the produced jets contain displaced vertices from B hadrons, though not all of these would be tagged in a real detector. Two of the four b -jets result from the decay of the Higgs boson h produced in the cascade decay of the \tilde{u}_L squark. In such an event, it may be possible to reconstruct the h mass, but with large errors compared to the mass reconstruction from the $h \rightarrow \gamma\gamma$ signal. This event also contains 380 GeV of E_T^{miss} from the undetected neutralinos and neutrinos produced in the cascade decays. We also remark that there are two

on-shell W bosons and an on-shell Z^0 boson in this event. Had the vector bosons decayed leptonically, they would have given rise to readily detectable hard electrons and muons that constitute the characteristic multilepton plus jet signature for SUSY.

A sample sparticle production event for a $\sqrt{s} = 500$ GeV linear e^+e^- collider is shown in Fig. 14.5. The event shown has $e^+e^- \rightarrow \tilde{W}_1^+ \tilde{W}_1^-$, where $\tilde{W}_1^+ \rightarrow u\bar{d}\tilde{Z}_1$ while $\tilde{W}_1^- \rightarrow e\bar{\nu}_e\tilde{Z}_1$. The electron track can be seen in the lower-right quadrant, where it deposits its energy in the EM calorimeter. The two quark jets are evident in the upper half plane. The event was generated in the mSUGRA model with parameters shown in the caption. The parameters are from the HB/FP region of mSUGRA parameter space (as discussed in Chapter 9), and give rise to a relic density $\Omega_{\tilde{Z}_1} h^2 = 0.11$, in accord with WMAP measurements.